

Optical Second Harmonic Generation in Achiral Bis(*n*-alkylamino)dicyanoquinodimethanes: Alkyl Chain Length as the Design Element

P. Gangopadhyay,[†] S. Sharma,[†] A. Jaganmohan Rao,[†] D. Narayana Rao,[‡] Shmuel Cohen,[§] Israel Agranat,^{||} and T. P. Radhakrishnan^{*,†}

School of Chemistry and School of Physics, University of Hyderabad, Hyderabad, India 500 046, and Department of Inorganic & Analytical Chemistry and Department of Organic Chemistry, The Hebrew University of Jerusalem, Jerusalem 91904, Israel

Received September 25, 1998

Chain length of substituted *n*-alkyl groups is proposed to be a convenient design element for the generation of noncentrosymmetric crystal lattices of interest in optical second harmonic generation (SHG). Powder studies on 7,7-Bis(*n*-alkylamino)-8,8-dicyanoquinodimethanes indicate that moderate solid-state optical SHG is obtained when the alkyl chains are of length 4, 5, and 6, and no detectable SHG occurs when the chains are of length 0, 3, 7, 8, and 12. The significant role of the intermediate alkyl chain length in generating noncentric crystal lattices is examined using the crystal structures of the propyl, butyl, and octyl derivatives presented in this paper.

Introduction

Assembly of molecules possessing large hyperpolarizability, β , into noncentrosymmetric bulk materials displaying strong quadratic nonlinear optical (NLO) effects such as optical second harmonic generation (SHG) is a topic of great current interest. A variety of molecular design strategies^{1–7} as well as physical techniques^{8,9} have been developed for this purpose. Incorporation of steric effects due to small groups such as methyl² or bulky groups with limited amphiphilic effect¹⁰ has been used to prepare crystals showing strong SHG; however, the potential of alkyl chains as crystal design elements for the fabrication of noncentric lattices with suitable alignment of NLO chromophores has not

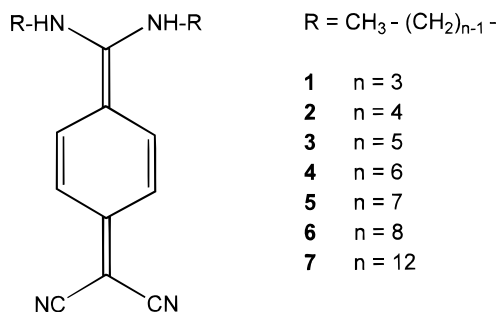


Figure 1. Molecular structure of the 7,7-bis(*n*-alkylamino)-8,8-dicyanoquinodimethanes studied.

been explored. Alkyl chains are easily attached to several active molecules and can strongly influence the crystal architecture. Alkyl chain interactions control bilayer structures in lipid membranes,¹¹ formation of LB films,¹² etc. and have been exploited in the 'molecular fastener' model for single component organic semiconductors.¹³ The latter is the only example that we are aware of where alkyl chains have been deliberately used as the design element in crystalline molecular materials.

We have considered the attachment of *n*-alkyl chains to strongly dipolar molecules and the variation of the chain length to control the dipole alignment. In systems with very short chains, the dominant Coulombic interactions would orient the molecular dipoles antiparallel and lead to centrosymmetric packing. When the chains are long, the strong interchain interactions could result in a bilayer structure with polar and nonpolar regions;¹⁴

* Corresponding author. E-mail: tprsc@uohyd.ernet.in. Fax: 91-40-3010120; Swarnajayant: Fellow of the Department of Science & Technology, New Delhi.

[†] School of Chemistry, University of Hyderabad.

[‡] School of Physics, University of Hyderabad.

[§] Department of Inorganic & Analytical Chemistry, The Hebrew University of Jerusalem.

^{||} Department of Organic Chemistry, The Hebrew University of Jerusalem.

(1) Zyss, J.; Chemla, D. S.; Nicoud, J.-F. *J. Chem. Phys.* **1981**, *74*, 4800.

(2) Lipscomb, G. F.; Garito, A. F.; Narang, R. S. *J. Chem. Phys.* **1981**, *75*, 1509.

(3) Oudar, L.; Hierle, R. *J. Appl. Phys.* **1977**, *84*, 2699.

(4) Marder, S. R.; Perry, J. W.; Narang, R. S. *Science* **1989**, *245*, 626.

(5) See the papers in *Chem. Mater.* **1994**, *6* (8).

(6) Sarma, J. A. R. P.; Allen, F. H.; Hoy, V. J.; Howard, J. A. K.; Thaimattam, R.; Biradha, K.; Desiraju, G. R. *J. Chem. Soc., Chem. Commun.* **1997**, 101.

(7) Zyss, J.; Oudar, L. *Phys. Rev.* **1982**, *A26*, 2028.

(8) Burland, D.; Miller, R. D.; Walsh, C. A. *Chem. Rev.* **1994**, *94*, 31.

(9) Ashwell, G. J.; Jefferies, G.; Hamilton, D. G.; Lynch, D. E.; Roberts, M. P. S.; Bahra, G. S.; Brown, C. R. *Nature* **1995**, *375*, 385.

(10) (a) Gunter, P.; Bosshard, Ch.; Sutter, K.; Arend, H.; Chapuis, G.; Tweig, R. J.; Dobrowolski, D. *Appl. Phys. Lett.* **1987**, *50*, 486. (b) Tomaru, S.; Matsumoto, S.; Kurihara, T.; Suzuki, H.; Ooba, N.; Kaino, T. *Appl. Phys. Lett.* **1991**, *58*, 2583.

(11) Pascher, I.; Lundmark, M.; Nyholm, P.; Sundell, S. *Biochim. Biophys. Acta.* **1992**, *1113*, 339.

(12) Schwartz, D. K. *Surf. Sci. Rep.* **1997**, *27*, 241.

(13) Inokuchi, H. *Int. Rev. Phys. Chem.* **1989**, *8*, 95.

(14) Bryan, R. F.; Hartley, P.; Miller, R. W.; Shen, M. *Mol. Cryst. Liq. Cryst.* **1980**, *62*, 281.

Table 1. Powder SHG Data for 2–4

particle size (μm)	2	3	4
100–150		8.0	8.0
150–200	12.9	9.6	12.0
200–250	15.1	10.0	12.0
250–300	17.2	10.0	10.0
300–350	19.4	14.0	12.8
350–420	19.4		
average SHG at saturation	18.7 at >250 μm	10.9 at >150 μm	11.7 at >150 μm

Table 2. Crystallographic Data for 2, 1, and 6

	2	1	6
molecular formula	$\text{C}_{18}\text{H}_{24}\text{N}_4$	$\text{C}_{16}\text{H}_{20}\text{N}_4$	$\text{C}_{26}\text{H}_{40}\text{N}_4$
space group	orthorhombic $Pna2_1$	monoclinic $C2/c$	monoclinic $C2/c$
<i>a</i> , Å	9.281(2)	20.667(8)	20.168(7)
<i>b</i> , Å	19.774(4)	9.158(6)	9.695(7)
<i>c</i> , Å	9.542(3)	18.302(4)	28.019(8)
α , deg	90.0	90.0	90.0
β , deg	90.0	112.93(2)	99.80(3)
γ , deg	90.0	90.0	90.0
<i>V</i> , Å ³	1751.2(8)	3190(2)	5398(5)
<i>Z</i>	4	8	8
ρ , g cm ⁻³	1.124	1.117	1.006
μ , cm ⁻¹	5.01 (Cu K α)	1.38 (Mo K α)	0.60 (Mo K α)
no. unique reflns	1845	2802	3512
no. of reflns with <i>I</i> > 2 σ <i>I</i>	1493	1674	1877
no. of paramtrs	216	192	258
<i>R</i> (for <i>I</i> > 2 σ <i>I</i>)	0.064	0.056	0.083
<i>R</i> _w / <i>wR</i> ²	0.087	0.151	0.272

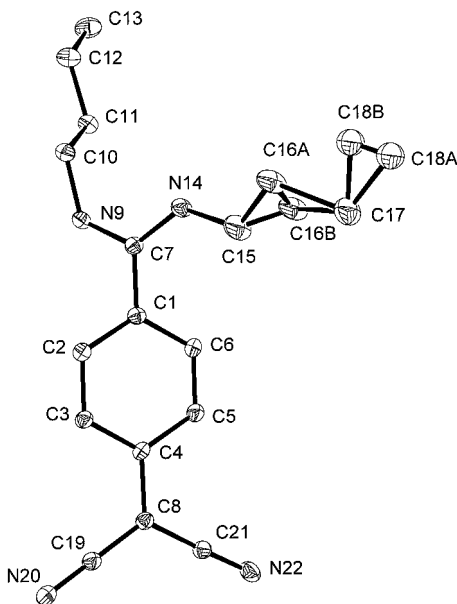


Figure 2. Molecular structure of **2** from single-crystal X-ray analysis; 10% probability ellipsoids are indicated; H atoms are omitted for clarity; the disorder in the position of C16 and C18 is indicated. The alkyl chains attached to N9 and N14 are referred to as A and B, respectively, in the text.

the Coulombic interactions within and between the polar regions would again encourage an antiparallel alignment of the molecular dipoles. At moderate chain lengths, the dipolar forces and alkyl chain interactions could be subtly balanced, leading to complex packing motifs; under such conditions the possibility of formation of noncentric crystal structures and dipole alignments of interest in quadratic NLO applications may be probed. Powder studies on alkyl-substituted *p*-nitroanilines (pNA)¹⁵ have shown that *N*-butyl-*p*-ni-

Table 3. (a) Fractional Atomic Coordinates and Equivalent Isotropic Displacement Parameters, (b) Significant Bond Lengths, and (c) Significant Bond Angles and Dihedral Angles in 2 from Single Crystal X-ray Analysis (Atom Labeling Shown in Figure 2)

Section a				
atom	<i>x</i>	<i>y</i>	<i>z</i>	<i>B</i> (eq)
C(1)	0.2794(4)	0.4169(2)	0.6000	4.6(2)
C(2)	0.2533(4)	0.4537(2)	0.7197(6)	4.9(2)
C(3)	0.3089(4)	0.5185(2)	0.7360(6)	4.7(2)
C(4)	0.3946(4)	0.5476(2)	0.6324(6)	4.4(1)
C(5)	0.4208(5)	0.5091(2)	0.5118(6)	5.1(2)
C(6)	0.3642(5)	0.4460(2)	0.4954(6)	5.3(2)
C(7)	0.2240(5)	0.3474(2)	0.5843(6)	4.8(2)
C(8)	0.4527(4)	0.6155(2)	0.6470(6)	4.6(2)
N(9)	0.2326(4)	0.3077(2)	0.6948(6)	5.1(1)
C(10)	0.1743(4)	0.2394(2)	0.7084(7)	5.4(2)
C(11)	0.2773(5)	0.1846(2)	0.6700(7)	5.4(2)
C(12)	0.2121(5)	0.1158(2)	0.6908(9)	6.8(2)
C(13)	0.3061(8)	0.0574(3)	0.656(1)	9.0(4)
N(14)	0.1680(5)	0.3247(2)	0.4675(6)	6.0(2)
C(15)	0.119(1)	0.3664(4)	0.349(1)	12.2(6)
C(16A) ^a	0.140(2)	0.3501(8)	0.230(2)	9.2(9)
C(16B) ^a	0.017(2)	0.3436(6)	0.260(2)	9.2(8)
C(17)	0.028(1)	0.3858(4)	0.114(1)	10.7(5)
C(18A) ^a	-0.065(3)	0.332(1)	0.086(4)	12(2).
C(18B) ^a	-0.065(3)	0.353(1)	0.011(3)	12(1).
C(19)	0.4250(5)	0.6552(2)	0.7633(7)	5.4(2)
N(20)	0.4016(6)	0.6881(2)	0.8612(7)	7.9(2)
C(21)	0.5366(5)	0.6434(2)	0.5400(6)	5.1(2)
N(22)	0.6057(5)	0.6649(2)	0.4491(7)	7.0(2)

Section b			
bond	distance (Å)	bond	distance (Å)
C(1)–C(2)	1.376(5)	C(7)–N(14)	1.309(6)
C(1)–C(7)	1.475(5)	C(8)–C(19)	1.383(6)
C(2)–C(3)	1.391(5)	C(8)–C(21)	1.398(6)
C(3)–C(4)	1.393(5)	N(9)–C(10)	1.460(5)
C(4)–C(5)	1.401(5)	N(14)–C(15)	1.471(8)
C(4)–C(8)	1.455(5)	C(19)–N(20)	1.158(6)
C(5)–C(6)	1.363(6)	C(21)–N(22)	1.159(6)
C(7)–N(9)	1.318(5)		

Section c			
bond	angle (deg)	bond	angle (deg)
C(2)–C(1)–C(6)	118.4(3)	C(1)–C(7)–N(9)	117.0(4)
C(2)–C(1)–C(7)	121.0(4)	C(1)–C(7)–N(14)	123.0(4)
C(6)–C(1)–C(7)	120.5(3)	N(9)–C(7)–N(14)	120.0(3)
C(1)–C(2)–C(3)	120.9(4)	C(4)–C(8)–C(19)	122.2(4)
C(2)–C(3)–C(4)	120.9(4)	C(4)–C(8)–C(21)	120.0(3)
C(3)–C(4)–C(5)	117.2(3)	C(19)–C(8)–C(21)	117.8(3)
C(3)–C(4)–C(8)	121.7(3)	C(7)–N(9)–C(10)	126.9(4)
C(5)–C(4)–C(8)	121.1(3)	C(7)–N(14)–C(15)	125.8(4)
C(4)–C(5)–C(6)	121.7(4)	C(8)–C(19)–N(20)	179.5(4)
C(1)–C(6)–C(5)	120.8(4)	C(8)–C(21)–N(22)	178.1(4)
C(6)–C(1)–C(7)–N(14)	-44.295	C(1)–C(7)–N(14)–C(15)	-15.839
C(2)–C(1)–C(7)–N(9)	-41.821	C(21)–C(8)–C(4)–C(5)	-0.192
C(1)–C(7)–N(9)–C(10)	174.370	C(19)–C(8)–C(4)–C(3)	-0.757

^a Occupancy 0.5.

troaniline has an SHG of approximately 12 U (1 U = SHG of urea) and that pNAs with shorter as well as longer alkyl chains are SHG inactive. These results and similar observations we have made in the case of diaminodicyanoquinodimethanes¹⁶ substituted with alkyl groups prompted us to explore, in detail, the model presented above.

We have recently demonstrated strong optical SHG in some chiral derivatives of diaminodicyanoquino-

(15) Chen, D.; Okamoto, N.; Matsushima, R. *Optics Commun.* **1989**, *69*, 425.

(16) Hertler, L. R.; Hartzler, H. D.; Acker, D. S.; Benson, R. E. *J. Am. Chem. Soc.* **1962**, *84*, 3387.

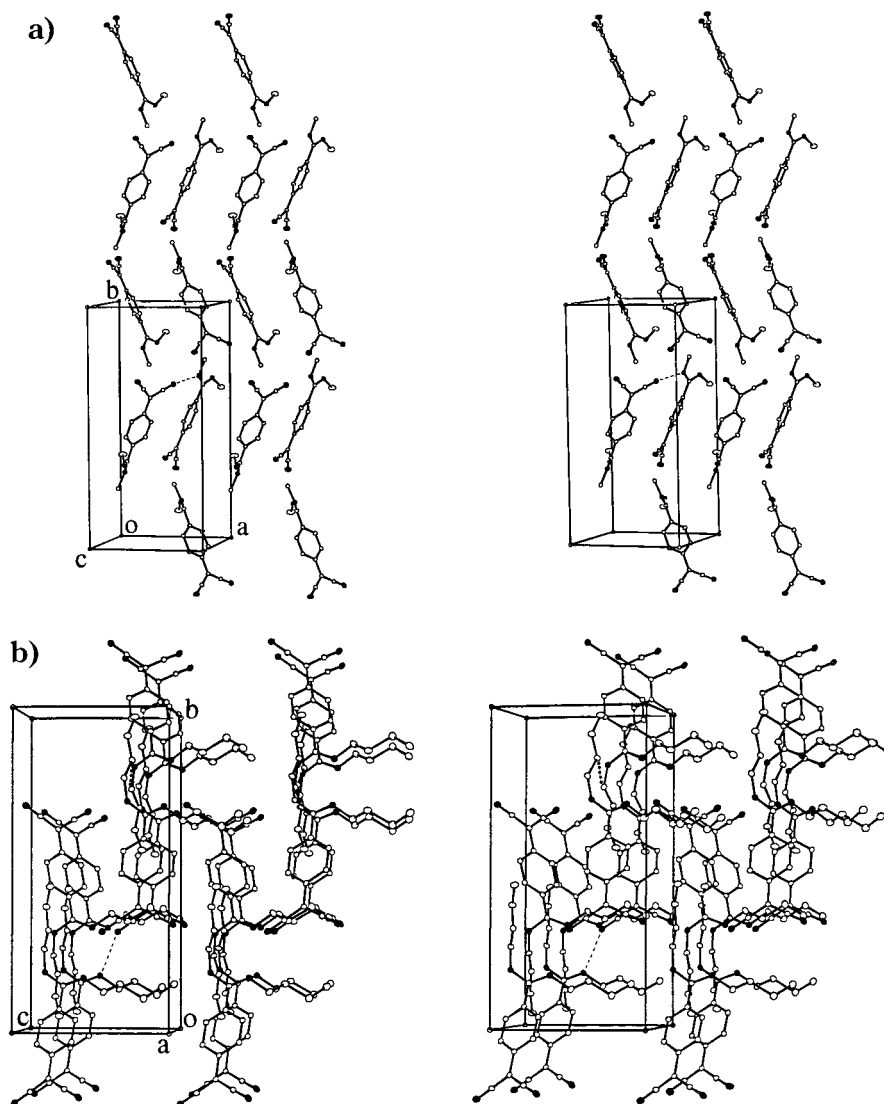


Figure 3. Crystal packing in **2**; the N atoms are shown as filled circles and H atoms are omitted for clarity. (a) Stereoview close to the c axis; in the butyl chains, only the C atoms attached to the amino N atom are shown; H-bond involving the N atom of the A chain, $r_{N9 \cdots N22'} = 2.855 \text{ \AA}$ (---), is indicated. (b) Stereoview along the a axis; only one of the positions of the disordered C atoms on the B chain is shown; H-bond involving the N atom of the B chain, $r_{N14 \cdots N20''} = 2.953 \text{ \AA}$ (---), and the closest C \cdots C interaction between the A chains, $r_{C10 \cdots C11''} = 3.996 \text{ \AA}$ (----), are indicated.

dimethane.¹⁷ Achiral derivatives of these strongly zwitterionic molecules have a dominant tendency to adopt centrosymmetric crystal structures.¹⁸ They also possess large hyperpolarizabilities [$\beta(0)$ values from AM1 calculation are from about -30 to -50×10^{-30} esu], good optical transparency, and thermal stability.¹⁷ Thus these molecules are ideal candidates to test the alkyl chain effect proposed above. We present in this paper a systematic study of the influence of alkyl chain length on the solid-state structure and optical SHG of 7,7-bis(*n*-alkylamino)-8,8-dicyanoquinodimethanes (Figure 1). The relevance of these results to the development of a new design technique for noncentrosymmetric crystal lattices of interest in quadratic NLO applications is noted.

Experimental Section

Synthesis and Characterization. All the compounds were synthesized following the procedure reported in ref 16. The detailed procedure is illustrated using the case of **2** as an example. A 0.200 g (0.98 mmol) portion of tetracyanoquinodimethane (TCNQ) was dissolved in 30 mL of freshly dried and distilled THF and warmed. A 0.4 mL (4 mmol) aliquot of freshly distilled *n*-butylamine was added (**Caution:** HCN gas is the biproduct in this reaction). The solution initially turned green and subsequently changed to dark purple-green; light yellow precipitate formation was also observed. It was stirred for 2–3 h and filtered. The filter cake was washed with dry ether and dried to give 0.257 g (89% yield) of **2**. It was recrystallized from methanol–water. Colorless transparent platelike crystals were grown from methanol–acetonitrile.

The synthesis of **5** was also carried out in THF; **1**, **3**, **4**, **6**, and **7** were synthesized in acetonitrile. **1**, **3**, **4**, **5**, **6**, and **7** were recrystallized from acetonitrile. The yields for the various compounds ranged from 60 to 90%.

7,7-Bis(propylamino)-8,8-dicyanoquinodimethane (1). Mp: 233–235 °C (dec). UV–vis (acetonitrile): $\lambda_{\text{max}} = 380 \text{ nm}$. FT-IR (KBr pellet): $\bar{\nu}/\text{cm}^{-1} = 3204.0$ (N–H stretch), 2181.7, 2135.4 (conjugated nitrile stretch). EI mass: $m/z = 268$ (M^+),

(17) (a) Ravi, M.; Rao, D. N.; Cohen, S.; Agranat, I.; Radhakrishnan, T. P. *J. Mater. Chem.* **1996**, *6*, 1119. (b) Ravi, M.; Rao, D. N.; Cohen, S.; Agranat, I.; Radhakrishnan, T. P. *Chem. Mater.* **1997**, *9*, 830.

(18) Ravi, M.; Cohen, S.; Agranat, I.; Radhakrishnan, T. P. *Struct. Chem.* **1996**, *7*, 225.

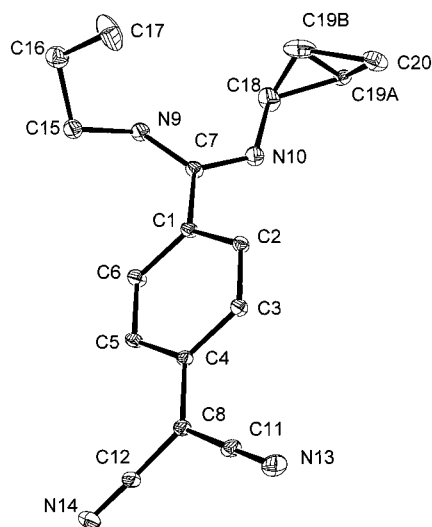


Figure 4. Molecular structure of **1** from single-crystal X-ray analysis; 10% probability ellipsoids are indicated; H atoms are omitted for clarity; the disorder in the position of C19 is indicated.

253, 239, 225, 182, 168, 58, 43. Elemental analysis (calcd for C₁₆H₂₀N₄): %C = 71.85 (71.64), %H = 7.65 (7.46), %N = 20.72 (20.90).

7,7-Bis(butylamino)-8,8-dicyanoquinodimethane (2). Mp: 270 °C (dec). UV-vis (acetonitrile): λ_{\max} = 365 nm. FT-IR (KBr pellet): $\bar{\nu}/\text{cm}^{-1}$ = 3196.3 (N-H stretch), 2183.6, 2137.3 (conjugated nitrile stretch). EI mass: m/z = 296 (M⁺). Elemental analysis (calcd for C₁₈H₂₄N₄): %C = 72.38 (72.94), %H = 8.01 (8.16), %N = 19.44 (18.90).

7,7-Bis(pentylamino)-8,8-dicyanoquinodimethane (3). Mp: 244–246 °C (dec). UV-vis (acetonitrile): λ_{\max} = 378 nm; FT-IR (KBr pellet): $\bar{\nu}/\text{cm}^{-1}$ = 3205.9 (N-H stretch), 2181.7, 2135.4 (conjugated nitrile stretch). EI mass: m/z = 324 (M⁺), 310, 296, 281, 239, 225, 182, 168. Elemental analysis (calcd for C₂₀H₂₈N₄): %C = 74.50 (74.03), %H = 8.61 (8.70), %N = 17.23 (17.27).

7,7-Bis(hexylamino)-8,8-dicyanoquinodimethane (4). Mp: 268 °C (dec). UV-vis (acetonitrile): λ_{\max} = 382 nm; FT-IR (KBr pellet): $\bar{\nu}/\text{cm}^{-1}$ = 3196.3 (N-H stretch), 2182.6, 2137.4 (conjugated nitrile stretch). EI mass: m/z = 353 (M⁺), 338, 324, 310, 296, 182, 168, 43. Elemental analysis (calcd for C₂₂H₃₂N₄): %C = 75.04 (74.96), %H = 9.05 (9.15), %N = 15.80 (15.89).

7,7-Bis(heptylamino)-8,8-dicyanoquinodimethane (5). Mp: 198–202 °C (dec). UV-vis (acetonitrile): λ_{\max} = 381 nm; FT-IR (KBr pellet): $\bar{\nu}/\text{cm}^{-1}$ = 3206.0 (N-H stretch), 2179.7, 2135.4 (conjugated nitrile stretch); FAB mass: m/z = 381 (M+1⁺), 185. Elemental analysis (calcd for C₂₄H₃₆N₄): %C = 75.90 (75.75), %H = 9.46 (9.53), %N = 14.78 (14.72).

7,7-Bis(octylamino)-8,8-dicyanoquinodimethane (6). Mp: 204–206 °C (dec). UV-vis (acetonitrile): λ_{\max} = 381 nm; FT-IR (KBr pellet): $\bar{\nu}/\text{cm}^{-1}$ = 3202.1 (N-H stretch), 2181.7, 2135.4 (conjugated nitrile stretch); FAB mass: m/z = 409 (M+1⁺), 408 (M⁺), 43. Elemental analysis (calcd for C₂₆H₄₀N₄): %C = 76.59 (76.42), %H = 9.65 (9.87), %N = 13.82 (13.71).

7,7-Bis(dodecylamino)-8,8-dicyanoquinodimethane (7). Mp: 216–222 °C (dec). UV-vis (acetonitrile): λ_{\max} = 378 nm; FT-IR (KBr pellet): $\bar{\nu}/\text{cm}^{-1}$ = 3196.0 (N-H stretch), 2181.7, 2137.3 (conjugated nitrile stretch); FAB mass: m/z = 521 (M+1⁺), 520 (M⁺), 43. Elemental analysis (calcd for C₃₄H₅₆N₄): %C = 78.72 (78.41), %H = 10.48 (10.83), %N = 10.95 (10.76).

Powder SHG Measurement. The powder SHG measurements were carried out using the Kurtz–Perry¹⁹ method. The fundamental wavelength (1064 nm) of a Q-switched Nd:YAG laser (Continuum, Model 660B-10) was used. The detection system consisted of a photomultiplier tube (Hamamatsu),

Table 4. (a) Fractional Atomic Coordinates and Equivalent Isotropic Displacement Parameters, (b) Significant Bond Lengths, and (c) Significant Bond Angles and Dihedral Angles in **1 from Single Crystal X-ray Analysis (Atom Labeling Shown in Figure 4)**

Section a				
atom	x	y	z	B(eq)
C(1)	0.3131	0.0676(3)	0.1433(1)	0.053(1)
C(2)	0.2680(1)	0.1862(3)	0.1134(2)	0.053(1)
C(3)	0.2093(1)	0.2027(3)	0.1293(2)	0.052(1)
C(4)	0.1923(1)	0.1031(3)	0.1774(1)	0.046(1)
C(5)	0.2380(1)	-0.0152(3)	0.2075(2)	0.058(1)
C(6)	0.2963(1)	-0.0327(3)	0.1901(2)	0.063(1)
C(7)	0.3794(1)	0.0551(3)	0.1320(2)	0.058(1)
C(8)	0.1309(1)	0.1212(3)	0.1961(2)	0.051(1)
N(9)	0.4002(1)	-0.0699(3)	0.1120(2)	0.069(1)
N(10)	0.4190(1)	0.1721(3)	0.1448(2)	0.079(1)
C(11)	0.0814(1)	0.2311(3)	0.1620(2)	0.058(1)
C(12)	0.1199(1)	0.0270(3)	0.2506(2)	0.061(1)
N(13)	0.0414(1)	0.3224(3)	0.1342(2)	0.085(1)
N(14)	0.1126(2)	-0.0520(3)	0.2958(2)	0.085(1)
C(15)	0.3563(2)	-0.1982(3)	0.0774(2)	0.075(1)
C(16)	0.3544(2)	-0.2339(5)	-0.0038(3)	0.091(1)
C(17)	0.3221(4)	-0.1155(6)	-0.0624(3)	0.164(3)
C(18)	0.4849(2)	0.1836(5)	0.1326(4)	0.114(2)
C(19A) ^a	0.4993(3)	0.3363(8)	0.1114(5)	0.061(3)
C(19B) ^b	0.4792(4)	0.2430(15)	0.0657(6)	0.122(5)
C(20)	0.4457(3)	0.4077(6)	0.0456(3)	0.110(1)

Section b			
bond	distance (Å)	bond	distance (Å)
C(1)–C(6)	1.388(4)	C(7)–N(10)	1.313(4)
C(1)–C(2)	1.397(3)	C(7)–N(9)	1.323(4)
C(1)–C(7)	1.468(3)	C(8)–C(11)	1.397(4)
C(2)–C(3)	1.364(3)	C(8)–C(12)	1.403(4)
C(3)–C(4)	1.404(4)	N(9)–C(15)	1.469(4)
C(4)–C(5)	1.402(4)	N(10)–C(18)	1.469(4)
C(4)–C(8)	1.446(3)	C(11)–N(13)	1.145(4)
C(5)–C(6)	1.371(4)	C(12)–N(14)	1.151(4)

Section c			
bond	angle (deg)	bond	angle (deg)
C(6)–C(1)–C(2)	117.88(18)	N(10)–C(7)–N(9)	120.5(2)
C(6)–C(1)–C(7)	120.5(2)	N(10)–C(7)–C(1)	117.5(2)
C(2)–C(1)–C(7)	121.4(2)	N(9)–C(7)–C(1)	121.9(2)
C(3)–C(2)–C(1)	121.1(2)	C(11)–C(8)–C(12)	117.9(2)
C(2)–C(3)–C(4)	121.5(2)	C(11)–C(8)–C(4)	122.3(2)
C(3)–C(4)–C(5)	116.9(2)	C(12)–C(8)–C(4)	119.9(2)
C(3)–C(4)–C(8)	122.0(2)	C(7)–N(9)–C(15)	126.7(2)
C(5)–C(4)–C(8)	121.0(2)	C(7)–N(10)–C(18)	125.6(3)
C(6)–C(5)–C(4)	121.2(2)	N(13)–C(11)–C(8)	179.3(3)
C(5)–C(6)–C(1)	121.3(2)	N(14)–C(12)–C(8)	178.2(3)
C(6)–C(1)–C(7)–N(9)	48.892	C(1)–C(7)–N(10)–C(18)	-176.717
C(2)–C(1)–C(7)–N(10)	45.293	C(11)–C(8)–C(4)–C(3)	5.774
C(1)–C(7)–N(9)–C(15)	17.879	C(12)–C(8)–C(4)–C(5)	5.943

^a Occupancy 0.4. ^b Occupancy 0.6.

oscilloscope (Tektronix, Model 2465B, 400 MHz) or lock-in amplifier (SRS, Model SR830), and personal computer. Powder samples were sandwiched between glass plates with the thickness of the sample controlled by 400 μm thick uniform Teflon sheets. Powder sizes were graded using standard sieves. Urea of particle size 100–150 μm was used as the standard, since at these particle sizes, the powder SHG of urea saturates at its maximum value. The errors in the measured SHGs are typically about 10–15%. All the compounds showed very good stability under laser irradiation and no sign of decomposition, even on continued irradiation with a laser power of 1 GW/cm² (6 ns, 10 Hz), was detected.

Crystal Structure Studies. X-ray diffraction data were collected on Enraf-Nonius CAD4 and MACH3 diffractometers. Cu K α or Mo K α radiation with a graphite crystal monochromator in the incident beam was used. Standard CAD4 centering, indexing, and data collection software was used. Details of data collection, solution and refinement, anisotropic thermal parameters, and bond lengths and angles are presented in the

(19) Kurtz, S. K.; Perry, T. T. *J. Appl. Phys.* **1968**, *39*, 3798; for details of our experimental procedure, see ref 17.

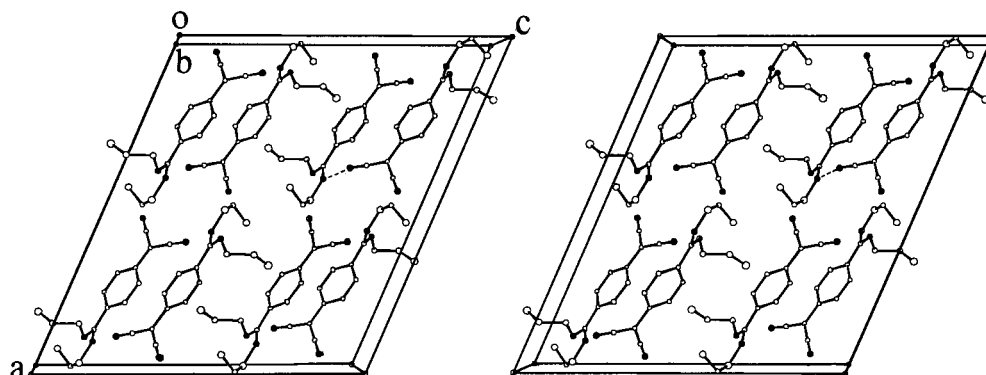


Figure 5. Crystal packing in **1**. Stereoview along the *b* axis; the N atoms are shown as filled circles and the H atoms are omitted for clarity; one of the two types of H-bond present, $r_{N10...N14} = 2.926 \text{ \AA}$ (---), is indicated.

Supporting Information.

Results and Discussion

The SHG capability of some amine-substituted TC-NQs has been investigated earlier.^{17,20} We have now synthesized the achiral 7,7-bis(*n*-alkylamino)-8,8-dicyanoquinodimethanes (Figure 1) with the alkyl groups propyl (**1**), butyl (**2**), pentyl (**3**), hexyl (**4**), heptyl (**5**), octyl (**6**), and dodecyl (**7**). Among these only **2** (7,7-bis(*n*-butylamino)-8,8-dicyanoquinodimethane) has been reported earlier along with the parent compound, 7,7-diamino-8,8-dicyanoquinodimethane (DADQ), and other derivatives.¹⁶ However the crystal structure and NLO properties of DADQ and **2** have not been investigated. Kurtz–Perry powder studies revealed no detectable SHG from DADQ, **1**, **5**, **6**, and **7**. However **2–4** showed moderate SHG; the intensity relative to urea measured for these compounds at various particle sizes is presented in Table 1. The SHG values of **2**, **3**, and **4** are found to reach saturation values of about 19, 11, and 12 U, respectively, at particle sizes typically above 150–250 μm , indicating phase-matchable behavior. These materials form transparent, colorless crystals with melting points typically around 250 $^{\circ}\text{C}$, hence they are of potential interest in device applications.

It is remarkable that strategies such as incorporation of chirality or dipole cancellation are not required to coax these strongly zwitterionic and achiral molecules away from a centrosymmetric arrangement. Interestingly a chiral compound similar to **2**, 7,7-bis((*S*)-2-methylbutylamino)-8,8-dicyanoquinodimethane, has been reported to show only weak (1 U) solid-state SHG.²¹ Introduction of simple *n*-alkyl chains of the right size without any involvement of chirality appears to be a promising strategy to induce noncentric crystal lattices. To investigate the impact of the chain length on the crystal packing, we have carried out single-crystal X-ray structure investigations on several of these compounds. Crystals of **1–3**, molecules with the shorter alkyl chains, gave good quality X-ray diffraction data. However, the longer alkyl chain derivatives, **4–6**, gave thin platelike crystals which provided relatively poor quality data, and

DADQ and **7** could not be crystallized at all. We present first the crystal structure of **2**, the SHG active material, and analyze the origin of the noncentrosymmetry in this crystal. It is then contrasted with the structures of the SHG inactive crystals **1** and **6**, having shorter and longer alkyl chains, respectively.

Colorless transparent plates of **2** grown from acetonitrile–methanol belong to *Pna2*₁ space group with one molecule in the asymmetric unit. The crystallographic data are collected in Table 2. The molecular structure is shown in Figure 2; the fractional atomic coordinates of non-hydrogen atoms, the significant bond lengths, and bond angles and dihedrals are collected in Table 3. The molecular structure is strongly benzenoid, indicating zwitterionic character, an effect arising from the electron-donating and -withdrawing groups. The diaminomethylene moiety is twisted out of the plane of the aromatic ring by approximately 43 $^{\circ}$, a feature common among these molecules.¹⁷ One of the butyl chains (A) is oriented antiperiplanar with respect to the ring (dihedral angle = 174.4 $^{\circ}$) and the other (B) synperiplanar (dihedral angle = –15.8 $^{\circ}$). The carbon atoms, which are second and fourth from the amino group on the B chain, showed disorder and were modeled using two positions with 50% probability of occupation. Figure 3a shows the crystal packing with molecular layers approximately parallel to the *ac* plane; the neighboring molecules are oriented with their major dipole axes (from the diaminomethylene carbon to the dicyanomethylene carbon) roughly antiparallel but with their aromatic ring planes at an angle of about 50.8 $^{\circ}$. The adjacent layers are slipped with respect to each other and show a zigzag orientation of the dipole axes. The view along the *a* axis (Figure 3b) reveals an interaction between A chains from adjacent layers; the shortest C...C distance is only 3.996 \AA . Interestingly, these chain interactions bring about a head-to-head orientation of the molecular dipoles in the adjacent layers. Two types of H-bonds are observed in **2** (Figure 3), connecting molecules into extended chains. We have also determined the crystal structure of SHG active **3**. It is found to belong to *Fdd2* space group, and the structure is very similar to that of **2**; hence, it is not discussed here. Because of the poor quality of the diffraction data, the structure of **4** could not be refined satisfactorily.

The molecular packing in **2** (and **3**) is controlled primarily by the dipole–dipole interactions between the zwitterions, the alkyl chain interactions and the H-bond

(20) (a) Lalama, S. J.; Singer, K. D.; Garito, A. F.; Desai, K. N. *Appl. Phys. Lett.* **1981**, *39*, 940. (b) Nicoud, J.-F.; Tweig, R. J. In *Nonlinear Optical Properties of Organic Molecules and Crystals*; Chmela, D. S., Zyss, J., Eds.; Academic Press: New York, 1987; Vol. 1, p 227; Vol. 2, p 221.

(21) Nicoud, J.-F. *Mol. Cryst. Liq. Cryst. Inc. Nonlin. Opt.* **1988**, *156*, 257.

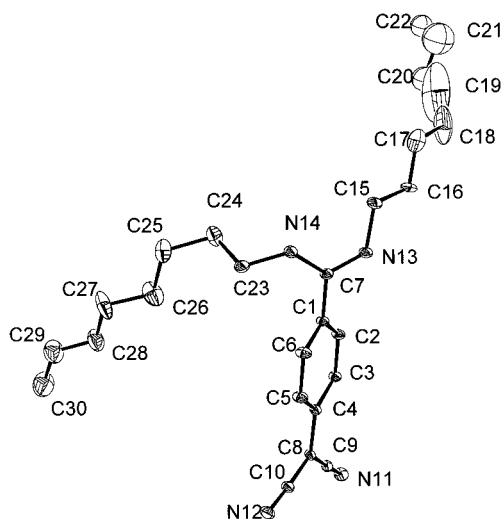


Figure 6. Molecular structure of **6** from single-crystal X-ray analysis; 5% probability ellipsoids are indicated; H atoms are omitted for clarity.

links between the amino H and cyano N atoms. The potential for dipole–dipole and H-bonding interactions are similar in the systems **1**–**8**. Therefore, the acentric crystal structures of the molecules with intermediate chain lengths point to the critical role of the alkyl chain interactions. The alkyl chains in these systems, while providing interlayer binding, appear to interfere with the dipolar interactions. The dipolar forces and inter-chain interactions that coexist and control the packing are supportive of the model we proposed above. Out of the interesting complexities that could result, a non-centric lattice has evolved in these cases, leading to the SHG activity.

These conclusions are strengthened by our analysis of the crystal structure of **1**. It is found to be centrosymmetric, belonging to $C2/c$ space group. The crystallographic data are collected in Table 2. The molecular structure is shown in Figure 4; the fractional atomic coordinates of non-hydrogen atoms, the significant bond lengths, and bond angles and dihedrals are collected in Table 4. The molecular structure of **1** is in many

respects similar to that of **2**, including the case of disorder in one of the alkyl chains. The disorder in the second C atom of one of the propyl chains was modeled using two positions of 40 and 60% probability of occupation. The crystal structure of **1** also shares several features with **2**, including the intermolecular H-bonding. However, the correlation between intermolecular layers in **1** is centrosymmetric and the net orientation of molecular dipoles is antiparallel, as seen from the crystal packing diagram (Figure 5). Significantly, no alkyl chain interactions are present, and the dipole–dipole interactions appear to be the dominant feature controlling the crystal packing. This shows that the alkyl chain interactions in **2** trigger the tilt of the molecular planes, the slippage of adjacent layers, the zigzag orientation of their dipoles, and the consequent breaking of the center of symmetry. An extra methylene unit on the alkyl chains has had a profound structural impact!

The structures of **1** and **2** reveal the transition in the crystal packing motif as the chain length changes from very short to medium size. To understand the transition once again to SHG inactive structures at longer alkyl chain lengths, it is necessary to examine the structure of **5**, **6**, or **7**. Crystals of **6** provided diffraction data which could be solved satisfactorily and refined to a large extent. **6** is also found to belong to $C2/c$ space group with one molecule in the asymmetric unit. The number of good quality data was not sufficient to model satisfactorily the disorder in the position of the atoms at the end of one of the alkyl chains; the last three carbons of this chain were refined isotropically while the rest of the non-hydrogen atoms in the molecule were refined anisotropically. The molecular structure is shown in Figure 6; the fractional coordinates of non-hydrogen atoms, the significant bond lengths, and angles are collected in Table 5. The crystal packing in **6** viewed along the *b* axis is presented in Figure 7. As in the case of **1** and **2**, intermolecular interactions involving the amino H atoms and cyano N atoms are observed in **6** as well. More significantly, it is seen that there is a quasi-bilayer type of packing present. The alkyl chain interactions are confined to alternating layers and the

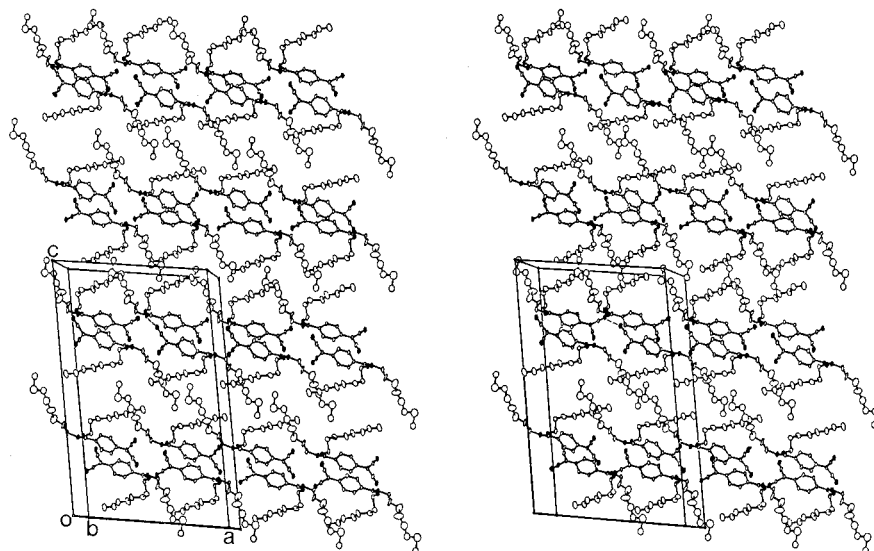


Figure 7. Crystal packing in **6**. Stereoview along the *b* axis; N atoms are shown as filled circles and H atoms are omitted for clarity; the H-bond present, $r_{N12...N13} = 2.957 \text{ \AA}$ (---), is indicated.

Table 5. (a) Fractional Atomic Coordinates and Equivalent Isotropic Displacement Parameters, (b) Significant Bond Lengths, and (c) Significant Bond Angles and Dihedral Angles in **6 from Single Crystal X-ray Analysis (Atom Labeling Shown in Figure 6)**

Section a				
atom	<i>x</i>	<i>y</i>	<i>z</i>	<i>B</i> (eq)
C(1)	0.3369(2)	0.7503(5)	0.1956(2)	0.089(2)
C(2)	0.2944(2)	0.6487(5)	0.1732(2)	0.099(2)
C(3)	0.2301(2)	0.6352(5)	0.1820(2)	0.092(2)
C(4)	0.2046(2)	0.7214(5)	0.2139(2)	0.087(1)
C(5)	0.2488(3)	0.8216(6)	0.2378(2)	0.113(2)
C(6)	0.3131(2)	0.8347(5)	0.2281(2)	0.113(2)
C(7)	0.4057(2)	0.7664(6)	0.1859(2)	0.097(2)
C(8)	0.1364(2)	0.7124(5)	0.2232(2)	0.094(2)
C(9)	0.0935(2)	0.6076(5)	0.2019(2)	0.098(2)
C(10)	0.1123(3)	0.8042(6)	0.2532(3)	0.113(2)
N(11)	0.0598(2)	0.5197(5)	0.1841(2)	0.129(2)
N(12)	0.0947(2)	0.8872(6)	0.2780(3)	0.141(2)
N(13)	0.4438(2)	0.6577(5)	0.1867(2)	0.116(2)
N(14)	0.4303(2)	0.8887(4)	0.1775(2)	0.115(2)
C(15)	0.5123(3)	0.6514(7)	0.1733(3)	0.158(3)
C(16)	0.5182(5)	0.5066(10)	0.1439(5)	0.254(7)
C(17)	0.5789(11)	0.4897(18)	0.1238(10)	0.406(14)
C(18)	0.5830(3)	0.3600(3)	0.0912(12)	0.560(3)
C(19)	0.6090(6)	0.3580(6)	0.0550(3)	1.000(2)
C(20)	0.6050(2)	0.3550(4)	0.0195(17)	0.520(3)
C(21)	0.6720(5)	0.3390(9)	0.0180(4)	0.790(7)
C(22)	0.6542(13)	0.3260(3)	-0.0368(10)	0.422(14)
C(23)	0.3916(3)	1.0144(7)	0.1644(3)	0.137(2)
C(24)	0.3940(6)	1.0573(12)	0.1138(4)	0.211(5)
C(25)	0.3542(8)	1.1928(12)	0.1000(5)	0.250(6)
C(26)	0.2796(7)	1.1859(15)	0.0968(7)	0.290(8)
C(27)	0.2418(9)	1.3124(14)	0.0789(7)	0.319(11)
C(28)	0.1758(8)	1.3067(14)	0.0728(7)	0.281(8)
C(29)	0.1372(9)	1.4144(19)	0.0557(8)	0.298(8)
C(30)	0.0708(9)	1.4150(2)	0.0464(8)	0.350(12)

Section b			
bond	distance (Å)	bond	distance (Å)
C(1)–C(6)	1.370(8)	C(8)–C(10)	1.369(9)
C(1)–C(2)	1.384(7)	C(8)–C(9)	1.400(8)
C(1)–C(7)	1.469(6)	N(11)–C(9)	1.151(7)
C(2)–C(3)	1.367(6)	N(12)–C(10)	1.158(8)
C(3)–C(4)	1.384(7)	N(13)–C(7)	1.302(6)
C(4)–C(5)	1.410(7)	N(13)–C(15)	1.494(7)
C(4)–C(8)	1.445(6)	N(14)–C(7)	1.321(6)
C(5)–C(6)	1.376(7)	N(14)–C(23)	1.460(8)

Section c			
bond	angle (deg)	bond	angle (deg)
C(7)–N(13)–C(15)	126.7(5)	C(6)–C(5)–C(4)	120.7(5)
C(7)–N(14)–C(23)	126.4(4)	C(1)–C(6)–C(5)	121.6(5)
C(6)–C(1)–C(2)	117.9(4)	N(13)–C(7)–N(14)	119.5(4)
C(6)–C(1)–C(7)	120.5(4)	N(13)–C(7)–C(1)	119.0(4)
C(2)–C(1)–C(7)	121.6(5)	N(14)–C(7)–C(1)	121.6(5)
C(3)–C(2)–C(1)	121.3(5)	C(10)–C(8)–C(9)	118.4(4)
C(2)–C(3)–C(4)	121.8(4)	C(10)–C(8)–C(4)	121.4(4)
C(3)–C(4)–C(5)	116.7(4)	C(9)–C(8)–C(4)	120.3(5)
C(3)–C(4)–C(8)	123.4(4)	N(11)–C(9)–C(8)	178.1(5)
C(5)–C(4)–C(8)	120.0(5)	N(12)–C(10)–C(8)	176.0(5)

molecular dipoles congregate in the layers in between. The chain interactions do not appear to interfere with the dipole–dipole interactions, as found in the case of **2**.

Thus we find a clear delineation of structural motifs as we progress from propyl to butyl to octyl chain substituted diaminodicyanoquinodimethanes. The three structures share several features at the molecular and crystal level. All the molecules show the peculiar extension of the two alkyl groups, with one being synperiplanar and the other antiperiplanar, as well as the twist

of the molecule about the bond connecting the diaminomethylene unit to the benzenoid ring. Intermolecular H-bonding is observed in all the systems. Therefore, variation in the packing of the crystals and consequently their NLO properties stem from the effect of the different alkyl chain lengths. The model we presented in the beginning is a convenient explanation of this effect.

Conclusion

The analysis of the crystal packing in **2**, **1**, and **6** clearly points to the important role played by the alkyl chain length in crystal packing. The alkyl chain interactions become noticeable in the butyl derivative onward and appear to become a significant force in the heptyl derivative and above in the diaminodicyanoquinodimethanes we have investigated; the lower melting points of **5**–**7** compared to that of **1**–**4** support this conclusion. In the short chain systems, the dipole–dipole interactions are the dominant force. In the medium-sized chain systems and in the longer chain systems, both alkyl chain interactions and dipole–dipole interactions coexist and the distinctions that lead to different crystal packing motifs are subtle. In the medium-sized alkyl chain systems such as **2**–**4**, the chain interactions interfere with the dipole alignments, leading to noncentric crystal lattices and SHG capability; this does not happen in the longer chain systems.

Crystallographic studies under way on pNA derivatives indicate that the *N*-butyl derivative is indeed noncentrosymmetric ($P2_12_12_1$ space group) and the *N*-propyl and *N*-pentyl derivatives are centrosymmetric ($P\bar{1}$ and $P2_1/c$ space groups, respectively). The general influence of the alkyl chain length is similar to that observed in the diaminodicyanoquinodimethanes; detailed structural studies on these derivatives will be published elsewhere. The present study of **2** and its homologues and the results on pNAs suggest a synthetically simple and versatile molecular engineering protocol for the design of noncentric molecular crystals of interest in NLO applications. Other NLO chromophores are being investigated to verify the generality of this approach.

Acknowledgment. Financial support from the CSIR and DST and the use of the National Single Crystal Diffractometer Facility funded by the DST at the School of Chemistry, University of Hyderabad are gratefully acknowledged. P.G. thanks the UGC for a Junior Research Fellowship.

Supporting Information Available: Details of crystal structure analysis and listing of atomic coordinates, thermal parameters, and bond distances and angles from X-ray crystal structure analysis for **2**, **1**, and **6**. This material is available free of charge via the Internet at <http://pubs.acs.org>.

CM980676H